JPET Fast Forward. Published on January 18, 2018 as DOI: 10.1124/jpet.117.245746
This article has not been copyedited and formatted. The final version may differ from this version.

JPET/2017/245746

Toll-like receptor 9-dependent AMPKα activation occurs via TAK1 and contributes to RhoA/ROCK signaling and actin polymerization in vascular smooth muscle cells

Cameron G. McCarthy, Camilla F. Wenceslau, Safia Ogbi, Theodora Szasz, and R. Clinton Webb

Department of Physiology, Augusta University, Augusta, GA, USA

Running title: TLR9-AMPKα signaling in vascular smooth muscle

Corresponding author:
Cameron G. McCarthy
Department of Physiology
Augusta University
1120 15th Street,
Augusta, GA, 30912
Phone: (706) 721-3547
Fax: (706) 721-7299
Email: cmccarthy@augusta.edu

Number of text pages: 37
Number of tables: 1
Number of figures: 6
Number of references: 50
Abstract word count: 249
Introduction word count: 484
Discussion word count: 1711

Non-standard abbreviations

1. ACC: Acetyl-CoA carboxylase
2. ACh: Acetylcholine
3. AMPKα: 5'-AMP-activated protein kinase α
4. CICR: Calcium-induced calcium release;
5. CpG: Cytosine-phosphate-guanine dinucleotides
6. eNOS: Endothelial nitric oxide synthase
7. ER: Endoplasmic reticulum
8. LKB1: Liver kinase B1
9. MRA: Mesenteric resistance arteries
10. MyD88: Myeloid differentiation primary response protein 88
11. MYPT1: Myosin phosphatase target subunit 1
12. NE: Norepinephrine
13. NF-κB: Nuclear factor kappa-light-chain-enhancer of activated B cells
14. ODN: Oligonucleotide
15. PE: Phenylephrine
16. PSS: Physiological salt solution
17. RhoGEFs: Rho guanine nucleotide exchange factors
18. ROCK: Rho-associated protein kinase
19. SERCA2: Sarco/endoplasmic reticulum Ca^{2+}-ATPase 2
20. TAK1: Transforming growth factor β-activated kinase 1

JPET Fast Forward. Published on January 18, 2018 as DOI: 10.1124/jpet.117.245746
This article has not been copyedited and formatted. The final version may differ from this version.

21. VSMCs: Vascular smooth muscle cells

Recommended section assignment: Cardiovascular

ABSTRACT

Traditionally, Toll-like receptor (TLR)9 signals through a MyD88-dependent cascade that results in pro-inflammatory gene transcription. Recently it was reported that TLR9 also participates in a stress tolerance signaling cascade in non-immune cells. In this non-canonical pathway, TLR9 binds to and inhibits sarco/endoplasmic reticulum Ca^{2+}-ATPase 2 (SERCA2), modulating intracellular calcium handling, and subsequently resulting in the activation of 5'-AMP-activated protein kinase (AMPK)α. We have previously reported TLR9 causes increased contraction in isolated arteries; however, the mechanisms underlying this vascular dysfunction need to be further clarified. Therefore, we hypothesized that non-canonical TLR9 signaling was also present in vascular smooth muscle cells (VSMCs) and that it mediates enhanced contractile responses through SERCA2 inhibition. To test these hypotheses, aortic microsomes, aortic VSMCs, and isolated arteries from male Sprague-Dawley rats were incubated with vehicle or TLR9 agonist (ODN2395). Despite clear AMPKα activation after treatment with ODN2395, SERCA2 activity was unaffected. Alternatively, ODN2395 caused phosphorylation of AMPKα via transforming growth factor β-activated kinase 1 (TAK1), a kinase involved in TLR9 inflammatory signaling. Downstream, we hypothesized that that TLR9 activation of AMPKα may be important in mediating actin cytoskeleton reorganization. ODN2395 significantly increased filamentous-to-globular actin ratio, as well as indices of RhoA/Rho-associated protein kinase (ROCK) activation, with the latter being prevented by AMPKα inhibition. In conclusion, AMPKα phosphorylation after TLR9 activation in VSMCs appears to be an extension of traditional inflammatory signaling via TAK1, as opposed to SERCA2 inhibition and the non-canonical pathway. Nonetheless, TLR9-AMPKα signaling can mediate VSMC function via RhoA/ROCK activation and actin polymerization.

INTRODUCTION

Components of the innate immune system have recently come to the fore as significant contributors to vascular dysfunction and subsequent cardiovascular disease (Bomfim et al., 2017). However, the mediators of this pathophysiological response, as well as the exact mechanisms of their actions, are still being revealed (Bomfim et al., 2017). The Toll-like receptor (TLR) family is a class of innate immune system pattern recognition receptors that has been implicated in the pathogenesis of various cardiovascular conditions (Goulopoulou et al., 2016; McCarthy et al., 2014). Of particular interest to our laboratory is TLR9, due to the elevated expression of its endogenous ligand, mitochondrial DNA, in different cardiovascular conditions (McCarthy et al., 2015; Oka et al., 2012; Veiko et al., 2010). We have recently reported that TLR9 is able to modulate vascular function and contribute to hypertension (McCarthy et al., 2015).

Toll-like receptor 9 has affinity for hypomethylated cytosine and guanine nucleotides separated by a phosphate-backbone (CpG). CpG dinucleotides are common to prokaryotic DNA but not eukaryotic DNA, and this specificity is important for preventing TLR9-dependent autoimmune responses (Stacey et al., 2003). In naïve cells, TLR9 is localized to the endoplasmic reticulum (ER) (Leifer et al., 2004), and upon cellular recognition of its ligand, it traffics through the Golgi to early endosomes and subsequently to endolysosomal compartments (Chockalingam et al., 2009; Latz et al., 2004).

Traditionally in immune cells, TLR9 upregulates inflammatory mediators by signaling through a myeloid differentiation primary response gene 88 (MyD88)-dependent pathway after trafficking from the ER to endolysosomes (Klinman, 2004). However recently, a “non-canonical” pathway for TLR9 was reported in cardiomyocytes and neurons (Shintani et al., 2013;

Shintani et al., 2014). In this pathway, retrograde transport of unmethylated CpG dinucleotides from endolysosomal compartments to the ER leads to the activation of uncleaved TLR9. TLR9 then directly inhibits the activity of sarco/endoplasmic reticulum Ca^{2+}-ATPase 2 (SERCA2). As a result of impaired calcium uptake into the ER, mitochondria calcium concentration decreases, leading to less mitochondrial ATP generation, and the resulting activation of 5'-AMP-activated protein kinase (AMPKα).

Given that calcium handling is important for vascular smooth muscle contraction and relaxation, TLR9 inhibition of SERCA2 could be a mechanism for the increased contractile responses and the vascular dysfunction that we have previously reported (McCarthy et al., 2015). Therefore, we hypothesized that (A) this non-canonical stress tolerance pathway for TLR9 is present in vascular smooth muscle cells (VSMCs) and (B) in isolated arteries (denuded of endothelium), TLR9 activation inhibits SERCA2 and this contributes to enhanced contractile responses. To test these hypotheses, aortic microsomes, aortic VSMCs, and isolated mesenteric resistance arteries (MRA) and aortae from male Sprague-Dawley rats were stimulated pharmacologically with a TLR9 agonist, ODN2395, and SERCA2 inhibition and AMPKα phosphorylation steps of non-canonical stress tolerance signaling pathway were explored. Elucidation of this non-canonical pathway in vascular smooth muscle may be important in cardiovascular conditions that involve TLR9 activation (Goulopoulou et al., 2016; McCarthy et al., 2014).

MATERIALS AND METHODS

Animals

Male Sprague Dawley rats (Envigo RMS, Indianapolis, IN, USA), 12-20 weeks old, were used for all experiments, including isolated arteries, primary VSMC cell culture, and vascular microsomes. All rats were maintained on a 12:12 hour light-dark cycle with both chow and water *ad libitium*. All procedures were performed in accordance with the Guide for the Care and Use of Laboratory Animals of the National Institutes of Health (NIH) and were reviewed and approved by the Institutional Animal Care and Use Committee of Augusta University.

Isolation of arteries

Rats were killed by thoracotomy and exsanguination via cardiac puncture under isoflurane anesthesia. Mesenteric resistance arteries (MRA) and thoracic aortae were removed from rats and placed in 4ºC physiological salt solution (PSS) containing: NaCl (130 mmol/L), $NaHCO_3$ (14.9 mmol/L), KCl (4.7 mmol/L), KH_2PO_4 (1.18 mmol/L), $MgSO_4 \cdot 7H_2O$ (1.18 mmol/L), $CaCl_2 \cdot 2H_2O$ (1.56 mmol/L), EDTA (0.026 mmol/L), and glucose (5.5 mmol/L) (all Sigma-Aldrich, St Louis, MO, USA). Excised arteries were cleaned of perivascular adipose tissue.

Cell culture

Primary VSMCs were cultured from the thoracic aortae using an enzymatic digestion method (McGuire et al., 1993). Cells were then grown in a humidified chamber at 37°C, with 5% CO_2, and low glucose Dulbecco's Modified Eagle's Medium (GE Healthcare, Logan, UT, USA) containing 10% fetal bovine serum (GE Healthcare) and 1% penicillin/streptomycin solution (Corning, Manassas, VA, USA). Treatments commenced between passages 3-6, when

culture dishes were ≥80% confluent. Twenty-four hours prior to treatments, cells were placed into serum-free media to achieve quiescence.

Isolation of vascular microsomes

Microsomes were extracted from pooled aortae (8/sample) via homogenization and differential ultracentrifugation, as previously described (Webb and Bhalla, 1976). Samples were resuspended in 50 μl of a specialized SERCA2 reaction solution containing: Tris-HCl (20 mmol/L), KCl (100 mmol/L), $MgCl_2$ (2 mmol/L), ATP (2 mmol/L), $CaCl_2$ (0.5 μmol/L), and oxalate (7.5 mmol/L) (all Sigma-Aldrich), pH 7.4.

Treatment

Isolated arteries in PSS, VSMCs in serum-free media, and microsomes in SERCA2 reaction solution were incubated for 20 minutes with either vehicle (endotoxin-free water; Invivogen, San Diego, CA, USA) or TLR9 agonist, type C synthetic CpG oligonucleotide ODN2395 (2 μmol/L; Invivogen). In some experiments, classical SERCA2 inhibitor thapsigargin (1 μmol/L; Tocris, Ellisville, MO, USA) was used as a positive control. To elucidate the signaling by which ODN2395 exerts its effects, different inhibitors were applied 30 min before vehicle or ODN2395. These included TLR9 antagonist, suppressive oligonucleotide ODN2088 (20 μmol/L; Invivogen); AMPKα inhibitor, compound C (10 μmol/L; EMD Millipore, Billerica, MA, USA); thapsigargin (1 μmol/L); transforming growth factor β-activated kinase 1 (TAK1) inhibitor, (57)-7-oxozeaenol (100 nmol/L; Tocris); vacuolar H^+-ATPase inhibitor, bafilomycin A1 (10 nmol/L; Tocris); and RhoA/ROCK inhibitor, Y-27632 dihydrochloride (1 μmol/L; Sigma-Aldrich).

Western blotting

Isolated arteries: After treatment, arteries were flash frozen in liquid nitrogen and homogenized in ice-cold tissue protein extraction reagent (T-PER; Thermo Fisher Scientific, Waltham, MA, USA), with protease inhibitors (sodium orthovanadate, phenylmethylsulfonyl fluoride, protease inhibitor cocktail) and phosphatase inhibitors (sodium fluoride and sodium pyrophosphate) (all Sigma-Aldrich).

Cell cultures: After treatment, cells were washed with an ice-cold phosphate-buffered saline (PBS) solution. Complete Lysis-M, including phosphatase inhibitor cocktail (PhosSTOP) (both Roche, Indianapolis, IN, USA), was then applied to each plate and allowed to remain on ice for 30 min. Cells were then harvested.

Protein concentration of both cell and tissue lysates was first determined and then equal quantities of protein (between 20-40 μg) were loaded into polyacrylamide gels (8-12%) and separated by sodium dodecyl sulfate polyacrylamide gel electrophoresis (SDS-PAGE). Gels were then transferred to polyvinylidene difluoride (PVDF) membranes (Thermo Fisher Scientific) and probed for protein expression (Table 1). Phosphorylated proteins were normalized to their total form, and β-actin was used as the loading control. Densitometric analysis was performed by Un-Scan-It (Version 6.1) (Silk Scientific, Orem, UT, USA).

Vascular function

Mesenteric resistance arteries were mounted on DMT wire myographs (Danish MyoTech, Aarhus, Denmark) and the endothelium was denuded by rubbing the lumen with a hair shaft. Arteries were then bathed in 37ºC PSS with 5% CO_2 and 95% O_2 and normalized to their optimal lumen diameter for active tension development, as described previously (McCarthy et al., 2015). Arteries were initially contracted to KCl (120 mmol/L) and endothelium integrity was then tested by the application of phenylephrine (PE; Sigma-Aldrich) (3 μmol/L) followed by

JPET Fast Forward. Published on January 18, 2018 as DOI: 10.1124/jpet.117.245746
This article has not been copyedited and formatted. The final version may differ from this version.

acetylcholine (ACh; Sigma-Aldrich) (3 μmol/L). Arteries were considered viable if KCl and PE contracted the arteries greater than 10 mN respectively, and endothelium denudation was considered successful if arteries relaxed less than 25% to ACh. Arteries then rested for 10 min, after which they were subjected to one of the following three protocols:

In PSS, MRA were first stimulated with PE (3 μmol/L). Upon plateau of the contractile response, the MRA were washed in calcium-free PSS+EGTA (Sigma-Aldrich) to deplete intracellular calcium stores for 20 min. During the depletion period, the MRA were also incubated with vehicle, ODN2395, or thapsigargin. After calcium depletion, intracellular calcium stores were loaded by placing the MRA in normal PSS (1.6 mmol/L calcium) for 15 min. Contractile responses during the loading period were taken as a functional measure of calcium influx (calcium loading). The bathing medium was then replaced again with calcium-free PSS (no EGTA). After 5 min, the MRA were stimulated with caffeine (Sigma-Aldrich) (20 mmol/L) to deplete intracellular calcium stores, which resulted in a transient contraction. The magnitude of this last response was taken as a measure of the ER to release calcium (intracellular calcium release). This protocol has been successfully employed in our laboratory (Giachini et al., 2009). Results are presented as percentage of the KCl contraction (%KCl).

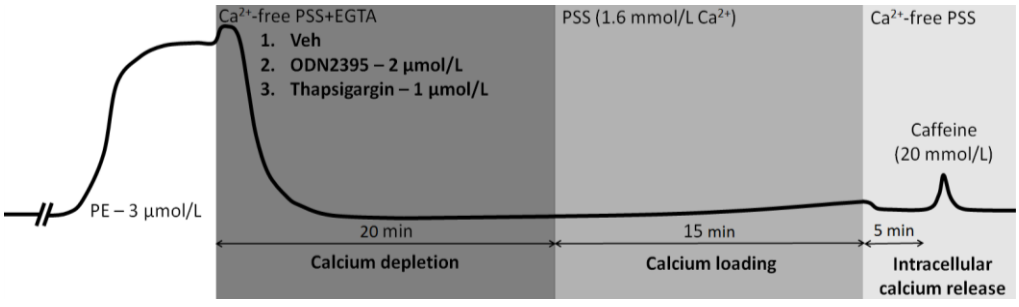

In PSS, MRA were first incubated with vehicle, ODN2395, or thapsigargin for 20 min. Then MRA were contracted with norepinephrine (NE; 3 μmol/L) (Sigma-Aldrich) and upon plateau, the PSS was washed one time and replaced. The time for contracted arteries to achieve

JPET Fast Forward. Published on January 18, 2018 as DOI: 10.1124/jpet.117.245746
This article has not been copyedited and formatted. The final version may differ from this version.

maximum relaxation was measured. This protocol has been successfully employed in our laboratory (Tostes et al., 1995). Results are presented in units of time (sec).

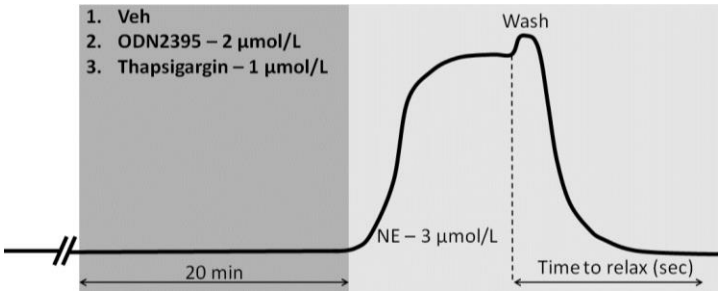

In PSS, MRA were first incubated with or without compound C for 30 min. Then MRA were incubated with vehicle or ODN2395 for a further 20 min. Finally, MRA were contracted with PE (10 µmol/L) and upon plateau, cumulative concentration-response curves were performed to Y-27632 (1 nmol/L-30 µmol/L). Results are presented as percent relaxation to the PE-induced contraction (%PE).

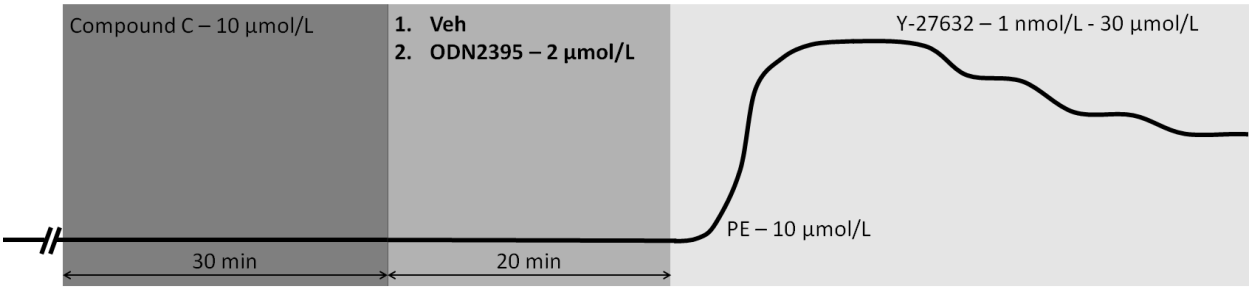

Luciferase assay

The activity of SERCA2 was also assessed using a luciferase assay in which ATP was quantified using an ATP Determination Kit (Invitrogen, Grand Island, NY, USA). This assay utilizes luciferase's requirement for ATP in producing light.

Protein concentration of isolated microsomes was determined and 35 µg of protein was incubated in a combined SERCA2 and luciferase reaction solutions. The SERCA2 reaction solution was as described above and the luciferase reaction solution was made according to manufacturer's instructions, with the exception of using the SERCA2 reaction solution instead of

deionized water. Microsomes were then subjected to treatment with vehicle or ODN2395, with and without thapsigargin. Luminescence was then read with a luminometer (BioTek, Winooski, VT, USA) at 5, 10, 20, 40, and 60 min and an ATP decay curve was constructed.

Co-immunoprecipitation

Endothelium-intact MRA were isolated, cleaned of perivascular adipose tissue, and pooled (2/sample). Homogenization was performed as described above for Western blotting. After protein concentration determination, 260 μg of protein was immunoprecipitated with either mouse anti-TLR9 (1:50; Abcam/ab12121, Cambridge, MA, USA) or rabbit anti-SERCA2 (1:50; Cell Signaling/4388, Danvers, MA, USA) for 2 h at 4°C, followed by incubation with Protein A/G PLUS-Agarose (Santa Cruz Biotechnology, Dallas, TX, USA) for another 24 h at 4°C. Samples were then washed 4 times with ice-cold T-PER with protease inhibitors and centrifuged at 1500 g for 5 min at 4°C after each wash. After the fourth wash, the supernatant was discarded and 50μl of 2X SDS sample buffer was added. Samples were then heated at 100°C for 10 min before being loaded into SDS-PAGE gels (7.5%) and transferred onto nitrocellulose membranes (Bio-Rad, Hercules, CA, USA). Finally, membranes were immunoblotted for the expression of SERCA2 (if TLR9 was immunoprecipitated) or TLR9 (if SERCA2 was immunoprecipitated) (both 1:1000 dilution).

Filamentous and globular actin quantification

Vascular smooth muscle cells were processed according to a G actin/F actin In Vivo Assay Kit (Cytoskeleton, Inc., Denver, CO, USA). Briefly, VSMCs were lysed in a detergent-based buffer that stabilizes the G and F forms of actin. Ultracentrifugation was then used to separate them – pelleting the F actin and leaving the G actin in the supernatant. After collecting the G actin, the F actin was depolymerized. Finally, the F and G actin samples were loaded into

polyacrylamide gels (10%), separated by SDS-PAGE, and transferred to PVDF membranes, as described above for Western blotting. Known quantities of actin control protein were included as standards. Densitometric analysis was performed by Un-Scan-It (Version 6.1) (Silk Scientific).

Confocal microscopy

To visualize F actin bundles and focal adhesion protein paxillin, VSMCs were grown in Lab-Tek II Chamber Slide w/Covers (Thermo Fisher Scientific) and confocal microscopy was performed. After treatment, VSMCs were fixed in 4% paraformaldehyde (Thermo Fisher Scientific) for 10 min and blocked in 1X PBS with 0.01% Triton X-100 (Thermo Fisher Scientific) and 5% horse serum. The slides were then incubated with rabbit anti-paxillin (1:100; Abcam/ab32084) primary antibody in 1X PBS and 5% bovine serum albumin (BSA) overnight. Next, slides were incubated with goat anti-rabbit IgG (H+L) cross-adsorbed secondary antibody Alexa Fluor 488 (1:200; Thermo Fisher Scientific/A-11008) and rhodamine phalloidin (1:40; Thermo Fisher Scientific/R415) in 1X PBS and 5% BSA for 90 min. Vectashield HardSet Antifade Mounting Medium with DAPI (H-1500) (Vector Laboratories, Inc., Burlingame, CA) was then applied to slides with coverslips. Vascular smooth muscle cells were visualized using a Zeiss LSM 780 Upright confocal microscope (63X objective) (Carl Zeiss MicroImaging, Oberkochen, Germany).

Statistical analysis

The sample size indicated per experiment (see figure legends) is the number of independent rats (or pooled samples) used, respective of treatment group. The statistical procedures used included one-way and two-way analysis of variances (ANOVAs) and Student's t-tests. Tukey's *post-hoc* testing was performed in the event of a significant one-way ANOVA

and a Bonferroni correction was used in the event of a significant two-way ANOVA. All analyses were performed using data analysis software GraphPad Prism 5.0 (La Jolla, CA). Statistical significance was set at $p<0.05$. The data are presented as mean ± SEM.

RESULTS

TLR9 activation increases vascular phospho-AMPKα^{Thr172} expression

To test our first hypothesis that the non-canonical stress tolerance signaling cascade is present in VSMCs, we probed for the expression of activated AMPKα, which is the ultimate step of the pathway (Shintani et al., 2013; Shintani et al., 2014). After pharmacologically activating TLR9 with ODN2395 (2 μmol/L), we observed that phospho-AMPKα^{Thr172} was significantly increased in isolated arteries (MRA, aorta, and endothelium denuded aorta), as well as VSMCs (Figure 1A-D). Importantly, pre-treatment of isolated arteries and VSMCs with TLR9 antagonist (ODN2088; 20 μmol/L) blocked this response, indicating that this increase in phospho-AMPKα^{Thr172} was specific to TLR9. Further supporting that ODN2395 activates AMPKα, we probed for the expression of phosphorylated acetyl-CoA carboxylase (ACC), which is one of the major enzymes regulated by AMPKα. We observed that ODN2395 significantly increased phospho-ACC^{Ser79} in VSMCs, and this increase was prevented by pre-treatment of the cells with an AMPKα inhibitor, compound C (10 μmol/L) (Figure 1E). Overall, these data suggest the presence of the non-canonical stress tolerance signaling cascade in VSMCs.

TLR9 activation does not impair SERCA2 activity, nor does it promote TLR9-SERCA2 colocalization

To further test for the presence of the non-canonical stress tolerance signaling cascade in VSMCs, we performed a series of SERCA2 activity assays, as inhibition of SERCA2 is an important early step in the pathway (Shintani et al., 2013; Shintani et al., 2014). Denuded MRAs were mounted on wire myographs to evaluate force development in response to calcium influx after depletion of intracellular calcium stores (calcium loading), and after caffeine (20 mmol/L) stimulation to measure the functional capacity of the ER to release calcium (intracellular calcium

release). During the calcium loading periods, force development was not different between vehicle and ODN2395, but it was increased by thapsigargin (positive control; 1 μmol/L) (%KCl, vehicle: 3.26±1.27 vs. ODN2395: 2.80±1.28 vs. thapsigargin: 10.23±2.51, *p<0.05) (Figure 2A). The magnitude of the contractile responses to caffeine were also not different between vehicle and ODN2395, but they were decreased by thapsigargin (%KCl, vehicle: 23.69±4.67 vs. ODN2395: 20.84±3.18 vs. thapsigargin: 2.04±0.53, *p<0.05) (Figure 2B). Similarly, the time for denuded MRA to reach maximum relaxation after contraction to NE was not different between vehicle and ODN2395, but it was increased by thapsigargin (Figure 2C). Overall, these vascular function data suggest that SERCA2 activity is not impaired when isolated MRA, denuded of endothelium, are treated with TLR9 agonist ODN2395.

To understand the contribution of TLR9 on SERCA2 activity at the molecular level, microsomes were isolated from pooled aortae. Microsomes are fragments of ER that we have previously extracted for analyzing SERCA2 activity and intracellular calcium sequestration (Webb and Bhalla, 1976). As SERCA2 is an ATPase, we used a luciferase assay to measure ATP concentration, and thapsigargin was applied as a pharmacological tool to obtain SERCA2 specificity. The presence of thapsigargin in both vehicle- and ODN2395-treated microsomes significantly increased the concentration of ATP at all time points (with the exception of 20 min ODN2395, which was trending, p=0.08) (Figure 2D). Area under the curve analysis of ATP decay across the 60 min of measurement revealed that ATP concentration in the vehicle incubated microsomes was low, indicative of ATP consumption with functional SERCA2 activity, and this significantly increased when vehicle incubated microsomes were pre-treated with thapsigargin [ATP concentration (AUC), vehicle: 19±3 vs. vehicle+thapsigargin: 140±35, *p<0.05]. Similarly, ATP concentration in ODN2395 incubated microsomes was low, and this

significantly increased when ODN2395 incubated microsomes were pre-treated with thapsigargin [ATP concentration (AUC), ODN2395: 22±9 vs. ODN2395+thapsigargin: 129±12, *p<0.05]. Importantly, no significant difference in ATP concentration was observed between vehicle- and ODN2395-treated microsomes (Figure 2E). To support these data, co-immunoprecipitation was performed for TLR9 with SERCA2, and vice versa, in MRA incubated with vehicle or ODN2395. Unlike Shintani et al. in cardiomyocytes (Shintani et al., 2014), there was no observable protein-protein interaction between TLR9 and SERCA2 in MRA stimulated with ODN2395 (Figure 2F). Finally, to support the mechanism that SERCA2 inhibition can induce AMPKα phosphorylation, we investigated whether classical SERCA2 inhibitor thapsigargin could increase phospho-AMPKα^{Thr172}. In isolated MRA, thapsigargin did not increase the expression of phospho-AMPKα^{Thr172} (Figure 2G). These experiments further reinforce that TLR9 activation with ODN2395 does not inhibit vascular smooth muscle SERCA2 activity and increases in cytosolic calcium concentration due to SERCA2 inhibition is insufficient to induce AMPKα phosphorylation in isolated arteries.

Inhibition of TAK1 prevents TLR9-dependent AMPKα^{Thr172} phosphorylation

Given that SERCA2 activity was not impaired by TLR9 activation with ODN2395, and that SERCA2 inhibition with thapsigargin did not increase phospho-AMPKα^{Thr172}, an alternative mechanism of AMPKα activation was pursued. Upon investigation of upstream kinases and activators of AMPKα, as well as canonical TLR9-inflammatory signaling, TAK1 was identified as a potential mediator of AMPKα phosphorylation (Momcilovic et al., 2006; Xie et al., 2006a). Accordingly, we observed that pre-treatment of VSMCs with TAK1 inhibitor (57)-7-oxozeaenol (100 nmol/L) prevented the ODN2395-dependent increase in phospho-AMPKα^{Thr172} (Figure 3A). Supporting these data, the activated form of TAK1, phospho-TAK1$^{Thr184/187}$, was significantly

JPET Fast Forward. Published on January 18, 2018 as DOI: 10.1124/jpet.117.245746
This article has not been copyedited and formatted. The final version may differ from this version.

increased after ODN2395 treatment compared to vehicle, and pre-treatment with ODN2088 blocked this response (Figure 3B). To corroborate that AMPK phosphorylation was coming from endolysosomal compartments, we pre-treated some VSMCs with vacuolar H^+-ATPase inhibitor bafilomycin A1 (10 nmol/L), which prevents endolysosome acidification, and therefore, TLR9 signaling specifically from the inflammatory canonical pathway. We observed that bafilomycin A1 also prevented the ODN2395-dependent increase in phospho-AMPKα^{Thr172} (Figure 3C), supporting the data with TAK1 inhibitor (57)-7-oxozeaenol. Interestingly, the phosphorylation of AMPKα in VSMCs appears to be a direct effect of TAK1, and not indirectly via liver kinase B1 (LKB1) (Figure 3D). Overall these data suggest that AMPKα is phosphorylated as a result of TLR9 inflammatory signaling (via TAK1) in VSMCs.

TLR9 increases actin polymerization and this is associated with AMPKα-RhoA/ROCK signaling

AMPKα is a multi-functional cell survival kinase, capable of regulating a number of cellular processes (Viollet et al., 2010), especially in the vasculature (Salt and Hardie, 2017). Given the vascular dysfunction we previously observed in rats treated with ODN2395 (McCarthy et al., 2015), we hypothesized that TLR9-AMPKα signaling may be inducing dysfunction via reorganization of the actin cytoskeleton (Miranda et al., 2010; Zheng and Cantley, 2007). Accordingly, we observed that ODN2395 treatment increases filamentous (F)-to-globular (G) actin ratio in VSMCs (Figure 4A). To support these quantitative data, we performed confocal microscopy on VSMCs after incubation with vehicle and ODN2395. Despite no obvious differences in the immunofluorescence of focal adhesion protein paxillin, the intensity of rhodamine-phalloidin staining, indicative of F actin, was clearly increased in VSMCs treated with ODN2395, and these F actin bundles also exhibited an element of disorganization compared to vehicle-treated VSMCs (Figure 4B).

JPET Fast Forward. Published on January 18, 2018 as DOI: 10.1124/jpet.117.245746
This article has not been copyedited and formatted. The final version may differ from this version.

Given that the Rho signaling governs global organization of F actin (Hall, 1998), we further hypothesized that ODN2395 increases RhoA/Rho-associated protein kinase (ROCK) activation via AMPKα to regulate actin polymerization. We observed that AMPKα inhibition with compound C increased the relaxation of vehicle-treated denuded MRA to RhoA/ROCK inhibitor Y-27632 (Figure 5A), indicating that RhoA/ROCK is activated by AMPKα in the basal condition of our vascular reactivity preparation. Similarly, compound C also potentiated the relaxation to Y-27632 in ODN2395-treated denuded MRA (Figure 5B), but this increase in relaxation occurred to a much greater extent (Figure 5C), indicating that RhoA/ROCK activation by AMPKα is increased after ODN2395 treatment. Supporting these vascular function data, Western blotting was performed for RhoA/ROCK substrate myosin phosphatase target subunit 1 (MYPT1), with the phosphorylated form of this protein being an indicator of active RhoA/ROCK signaling. We observed that ODN2395 significantly increased phospho-MYPT1^{Thr696} in VSMCs, and this increase was prevented by pre-treatment of the cells with compound C (Figure 5D).

Cofilin is an actin severing protein that can depolymerize actin filaments. Therefore, its inactivation via phosphorylation, which can be modulated by ROCK (Maekawa et al., 1999), stabilizes F actin and promotes its accumulation (Moon and Drubin, 1995). Therefore, we hypothesized that TLR9 activation with ODN2395 would increase cofilin phosphorylation, thereby abrogating its activity. We observed that ODN2395 significantly increased phospho-cofilin^{Ser3} in VSMCs, and this increase was prevented by pre-treatment of the cells with Y-27632 (1 μmol/L) (Figure 5E). Interestingly, Y-27632 also lowered the phospho-cofilin^{Ser3} expression in our vehicle-treated VSMCs, again suggesting that that RhoA/ROCK is activated to a small degree in the basal condition of our cell culture preparation (Figure 5E).

DISCUSSION

The present investigation reveals three significant discoveries surrounding TLR9 signaling in VSMCs. The first major finding was that AMPKα activation downstream of TLR9 appears to be an extension of canonical inflammatory signaling via TAK1. Secondly, the non-canonical stress tolerance signaling cascade for TLR9, that is initiated by SERCA2 inhibition and that has been reported in cardiomyocytes and neurons, is not present in VSMCs. Finally, TLR9-AMPKα signaling can activate RhoA/ROCK and promote the accumulation of F actin (Figure 6). These data support a novel mechanism by which TLR9 can impact vascular function and potentially contribute to the pathogenesis of cardiovascular diseases (Goulopoulou et al., 2016; McCarthy et al., 2014).

Previously, we have reported that arteries from rats treated *in vivo* with TLR9 agonist ODN2395 present significant dysfunction (McCarthy et al., 2015). These data add to the growing body of literature illustrating that activation of almost all TLRs (including those located on endosomes and the plasma membrane) can impact vascular function through various mechanisms (Goulopoulou et al., 2016; McCarthy et al., 2014). Given the well-established role of TLRs, including TLR9, in vascular (patho)physiology, in the present study we wanted to understand further the mechanisms underlying TLR9-dependent vascular dysfunction, and specifically whether TLR9 activation inhibits vascular smooth muscle SERCA2 and contributes to enhanced contractile responses.

In order to fully understand the significance and novelty of the TLR9 non-canonical signaling cascade reported by Shintani et al. (Shintani et al., 2013; Shintani et al., 2014), one must understand the multistep, tightly regulated processing prior to canonical TLR9 (inflammatory) activation (Goulopoulou et al., 2016). In contrast, the TLR9 non-canonical

signaling pathway was reported to cause SERCA2 inhibition and ultimately resulted in AMPKα activation. In the current investigation, regardless of our experimental approach (isolated arteries *ex vivo* and aortic microsomes *in vitro*), we were not able to observe any evidence of SERCA2 inhibition after treatment with TLR9 agonist ODN2395. Despite the lack of effect on SERCA2 activity, we observed clear AMPKα phosphorylation at its activation site, threonine 172, suggesting that AMPKα activation downstream of TLR9 was occurring through some other mechanism. Supporting an alternative mechanism was the observation that SERCA2 inhibition with thapsigargin was also not sufficient to induce AMPKα phosphorylation in isolated MRA, unlike TLR9 agonist ODN2395. Therefore, an alternative upstream kinase of AMPKα was investigated. Given that TAK1 has been identified as an activator of AMPKα (Viollet et al., 2010), as well as a kinase involved in canonical TLR9-inflammatory signaling (Vollmer, 2006), it seemed logical that TAK1 was the kinase phosphorylating AMPKα after ODN2395 treatment. TAK1 is a member of the mitogen-activated kinase kinase kinase family (Ninomiya-Tsuji et al., 2003) and it induces inflammation by activating both p38 and nuclear factor kappa-light-chain-enhancer of activated B cells (NF-κB) (Ninomiya-Tsuji et al., 1999; Sakurai et al., 1999), both of which we have observed in arteries from rats treated with ODN2395 (McCarthy et al., 2015). Moreover, TAK1 also serves as a key regulator of TLR9 signaling in B lymphocytes (Szili et al., 2014) and is also known to regulate AMPKα phosphorylation in cardiac cells (albeit via LKB1, which we did not observe) (Xie et al., 2006b) and endothelial cells (Zippel et al., 2013). Therefore, we conclude that the mechanism of AMPKα phosphorylation after TLR9 activation with ODN2395 in VSMCs is an extension of inflammatory signaling via TAK1 and not the non-canonical stress tolerance signaling cascade.

Why the non-canonical stress tolerance signaling cascade for TLR9 is specialized to cardiomyocytes and neurons and not conserved across all non-immune cells is unknown. Physiologically, we hypothesize that one possible reason could be due to the mechanism by which SERCA2 contributes to vascular smooth muscle contraction, which is different from cardiomyocytes. As cardiac contractions are rapid and of short duration, contractile responses are severely diminished after SERCA2 inhibition, illustrating the importance of store-operated calcium entry to normal cardiac function (MacLennan and Kranias, 2003). On the other hand, vascular smooth muscle contraction is relatively slow, in some cases sustained and tonic, and therefore, inhibition of SERCA2 in vascular smooth muscle promotes contraction by increasing the concentration of calcium that can bind with calmodulin and activate myosin light chain kinase. In turn, calcium, through the process of calcium-induced calcium release (CICR), activates the ryanodine receptor leading to calcium release from the sarcoplasmic reticulum. Unlike cardiomyocytes, where calcium entry is further amplified through CICR, this process seems to be locally restricted to a few subplasmalemmal calcium sparks sites in VSMCs (House et al., 2008; Kamishima and Quayle, 2003).

Experimentally, we utilized a type C TLR9 agonist (ODN2395) in the present investigation, whereas Shintani *et al.* used type A and type B ODNs (Shintani et al., 2013; Shintani et al., 2014). Type A ODNs induce a strong interferon response but only weakly stimulate NF-κB, whereas type B ODNs induce a strong NF-κB response but only weakly stimulate interferons (Vollmer and Krieg, 2009). Type C ODNs combine the immunogenicity of both type A and type B ODNs (Vollmer and Krieg, 2009), and also have a complete phosphorothioated backbone, which makes them more resistant to nuclease degradation (Roberts et al., 2011). Based on the combined immunogenicity of ODN2395 and the fact that Shintani *et*

al. used type A and type B ODNs to support their data (Shintani et al., 2013; Shintani et al., 2014), it does not appear that differences in TLR9 agonist choice explains the confounding data between the two studies.

Similarly, we also acknowledge the temporal differences of AMPKα phosphorylation (Thr172) between our study and those of Shintani *et al.* (Shintani et al., 2013; Shintani et al., 2014). In cardiomyocytes, Shintani *et al.* observed increases in phospho-AMPKα^{Thr172} as early as 10 min after TLR9 activation. Nonetheless, this increase only reached statistical significance at the 30, 60 (peak phosphorylation), and 120 min time points. In our previous publication (McCarthy et al., 2015), we observed significant increases in phospho-AMPKα^{Thr172} at 15 and 30 min after TLR9 activation in isolated MRA. Based on these data, 20 min was chosen as a single time point in the present study. It does not appear that we missed activation of the non-canonical stress tolerance signaling cascade for TLR9 because our luciferase assay incorporated a time course (5, 10, 20, 40, and 60 min) and no difference in ATP concentration, and thus SERCA2 activity, was observed between vehicle- and ODN2395-treated microsomes.

Regardless of its mechanism of activation, AMPKα is recognized to have multiple effects on vascular function (Salt and Hardie, 2017). As a serine-threonine kinase protein complex that is a central regulator of cellular energy homeostasis, there is an abundance of literature demonstrating that AMPKα has anti-contractile-pro-relaxant properties (Ewart and Kennedy, 2011; Garcia-Prieto et al., 2015), including phosphorylation of endothelial nitric oxide synthase (eNOS) at the activation site serine 1177 (Chen et al., 1999; Morrow et al., 2003), as well as mechanisms that are independent of the endothelium (Davis et al., 2012; Horman et al., 2008; Pyla et al., 2014; Sung and Choi, 2012). However, there are instances when AMPK induces vascular dysfunction (Turkseven and Ertuna, 2013), and AMPKα is also known to phosphorylate

eNOS at threonine 495 in the calcium-calmodulin-binding sequence, resulting in the inhibition of eNOS activity (Chen et al., 1999). Given the clear phosphorylation of AMPKα (Thr172), in conjunction with heightened contractile responses we previously reported in rats treated with ODN2395 (McCarthy et al., 2015), and our original focus in the current manuscript on vascular smooth muscle contraction, we hypothesized that TLR9-AMPKα signaling may be mediating actin cytoskeleton reorganization (Miranda et al., 2010; Zheng and Cantley, 2007), particularly in vascular smooth muscle. Nonetheless, it is interesting to postulate why TLR9-dependent activation of AMPKα abrogates its positive effects on vascular function, particularly in conditions when the endothelium is present, such as our *in vivo* model (McCarthy et al., 2015). In addition to the potential for cytoskeleton reorganization in endothelial cells (thus, impairing the barrier function of the endothelium), we also hypothesize that the concurrent generation of reactive oxygen species and/or pro-inflammatory cytokines downstream of TLR9 is causing AMPKα to become dysregulated. Specific experiments will be required to test these hypotheses in future studies.

It is well known that RhoA through serine-threonine kinase ROCK mediates VSMC function by calcium-sensitization (maintaining the activity of myosin light-chain kinase, independently of free cytosolic calcium) and cytoskeleton reorganization (Nunes et al., 2010). In our vascular reactivity experiments, pre-contraction to α_1-adrenergic agonists were not different in arteries incubated with vehicle or ODN2395 (data not shown), and surprisingly, the magnitude of relaxation to Y-27632 was not different between vehicle and ODN2395. Therefore, we can infer that the potentiated relaxation of denuded MRA to Y-27632 after incubation with ODN2395 and compound C is due to a decrease in F actin formation, as opposed to an inhibition of calcium-sensitization and contractility.

In this investigation we observed that AMPKα can activate RhoA/ROCK signaling in VSMCs, similar to what has been observed in kidney epithelial cells (Miranda et al., 2010). It is well established that the Rho family GTPases are key regulators of cytoskeleton organization, with the GTPase RhoA controlling stress fiber formation and actin polymerization (Hall, 1998). ROCK interacts with RhoA, and the two substrates of this kinase, myosin light chain phosphatase and myosin light chain, can regulate the assembly of actin-myosin filament bundles (Hall, 1998). While ROCK does not directly phosphorylate actin severing protein cofilin, it is able to phosphorylate LIM-kinase, which in turn phosphorylates and inactivates cofilin (Maekawa et al., 1999) and thus promotes the stabilization and accumulation of F actin (Moon and Drubin, 1995), which is what we observed in our study. Overall these data add to the growing body of literature suggesting that ROCK can be activated via mechanisms other than Rho guanine nucleotide exchange factors (RhoGEFs) (Boulter et al., 2012).

In conclusion, the current investigation reveals a novel mechanism by which TLR9 contributes to the pathogenesis of cardiovascular diseases (Goulopoulou et al., 2016; McCarthy et al., 2014). While this mechanism did not involve changes in calcium handling via SERCA2 inhibition like originally hypothesized, it did involve modulating actin cytoskeleton organization, which could then contribute to reduced vasodilation and decreased blood flow to end organs. These data further emphasize the far reaching effects of immune system activation in (patho)physiology, especially in tissues, which in many cases, are the first to respond to perturbations in homeostasis (Matzinger and Kamala, 2011).

AUTHOR CONTRIBUTIONS

Participated in research design: McCarthy, Wenceslau, Szasz, and Webb

Conducted experiments: McCarthy, Wenceslau, and Ogbi

Performed data analysis: McCarthy

Wrote or contributed to the writing of the manuscript: McCarthy, Wenceslau, Szasz, and Webb

REFERENCES

Bomfim GF, Rodrigues FL, Carneiro FS. (2017) Are the innate and adaptive immune systems setting hypertension on fire? *Pharmacol Res* **117**:377-393.

Boulter E, Estrach S, Garcia-Mata R, Feral CC. (2012) Off the beaten paths: Alternative and crosstalk regulation of rho GTPases. *Faseb J* **26**:469-479.

Chen ZP, Mitchelhill KI, Michell BJ, Stapleton D, Rodriguez-Crespo I, Witters LA, Power DA, Ortiz de Montellano PR, Kemp BE. (1999) AMP-activated protein kinase phosphorylation of endothelial NO synthase. *FEBS Lett* **443**:285-289.

Chockalingam A, Brooks JC, Cameron JL, Blum LK, Leifer CA. (2009) TLR9 traffics through the golgi complex to localize to endolysosomes and respond to CpG DNA. *Immunol Cell Biol* **87**:209-217.

Davis B, Rahman A, Arner A. (2012) AMP-activated kinase relaxes agonist induced contractions in the mouse aorta via effects on PKC signaling and inhibits NO-induced relaxation. *Eur J Pharmacol* **695**:88-95.

Ewart MA and Kennedy S. (2011) AMPK and vasculoprotection. *Pharmacol Ther* **131**:242-253.

Garcia-Prieto CF, Gil-Ortega M, Aranguez I, Ortiz-Besoain M, Somoza B, Fernandez-Alfonso MS. (2015) Vascular AMPK as an attractive target in the treatment of vascular complications of obesity. *Vascul Pharmacol* **67-69**:10-20.

Giachini FR, Chiao CW, Carneiro FS, Lima VV, Carneiro ZN, Dorrance AM, Tostes RC, Webb RC. (2009) Increased activation of stromal interaction molecule-1/orai-1 in aorta from hypertensive rats: A novel insight into vascular dysfunction. *Hypertension* **53**:409-416.

Goulopoulou S, McCarthy CG, Webb RC. (2016) Toll-like receptors in the vascular system: Sensing the dangers within. *Pharmacol Rev* **68**:142-167.

Hall A. (1998) Rho GTPases and the actin cytoskeleton. *Science* **279**:509-514.

Horman S, Morel N, Vertommen D, Hussain N, Neumann D, Beauloye C, El Najjar N, Forcet C, Viollet B, Walsh MP, Hue L, Rider MH. (2008) AMP-activated protein kinase phosphorylates and desensitizes smooth muscle myosin light chain kinase. *J Biol Chem* **283**:18505-18512.

House SJ, Potier M, Bisaillon J, Singer HA, Trebak M. (2008) The non-excitable smooth muscle: Calcium signaling and phenotypic switching during vascular disease. *Pflugers Arch* **456**:769-785.

Kamishima T and Quayle JM. (2003) Ca2+-induced Ca2+ release in cardiac and smooth muscle cells. *Biochem Soc Trans* **31**:943-946.

Klinman DM. (2004) Immunotherapeutic uses of CpG oligodeoxynucleotides. *Nat Rev Immunol* **4**:249-258.

Latz E, Schoenemeyer A, Visintin A, Fitzgerald KA, Monks BG, Knetter CF, Lien E, Nilsen NJ, Espevik T, Golenbock DT. (2004) TLR9 signals after translocating from the ER to CpG DNA in the lysosome. *Nat Immunol* **5**:190-198.

Leifer CA, Kennedy MN, Mazzoni A, Lee C, Kruhlak MJ, Segal DM. (2004) TLR9 is localized in the endoplasmic reticulum prior to stimulation. *J Immunol* **173**:1179-1183.

MacLennan DH and Kranias EG. (2003) Phospholamban: A crucial regulator of cardiac contractility. *Nat Rev Mol Cell Biol* **4**:566-577.

Maekawa M, Ishizaki T, Boku S, Watanabe N, Fujita A, Iwamatsu A, Obinata T, Ohashi K, Mizuno K, Narumiya S. (1999) Signaling from rho to the actin cytoskeleton through protein kinases ROCK and LIM-kinase. *Science* **285**:895-898.

Matzinger P and Kamala T. (2011) Tissue-based class control: The other side of tolerance. *Nat Rev Immunol* **11**:221-230.

McCarthy CG, Goulopoulou S, Wenceslau CF, Spitler K, Matsumoto T, Webb RC. (2014) Toll-like receptors and damage-associated molecular patterns: Novel links between inflammation and hypertension. *Am J Physiol Heart Circ Physiol* **306**:H184-96.

McCarthy CG, Wenceslau CF, Goulopoulou S, Ogbi S, Baban B, Sullivan JC, Matsumoto T, Webb RC. (2015) Circulating mitochondrial DNA and toll-like receptor 9 are associated with vascular dysfunction in spontaneously hypertensive rats. *Cardiovasc Res* **107**:119-130.

McGuire PG, Walker-Caprioglio HM, Little SA, McGuffee LJ. (1993) Isolation and culture of rat superior mesenteric artery smooth muscle cells. *In Vitro Cell Dev Biol* **29A**:135-139.

Miranda L, Carpentier S, Platek A, Hussain N, Gueuning MA, Vertommen D, Ozkan Y, Sid B, Hue L, Courtoy PJ, Rider MH, Horman S. (2010) AMP-activated protein kinase induces actin cytoskeleton reorganization in epithelial cells. *Biochem Biophys Res Commun* **396**:656-661.

Momcilovic M, Hong SP, Carlson M. (2006) Mammalian TAK1 activates Snf1 protein kinase in yeast and phosphorylates AMP-activated protein kinase in vitro. *J Biol Chem* **281**:25336-25343.

Moon A and Drubin DG. (1995) The ADF/cofilin proteins: Stimulus-responsive modulators of actin dynamics. *Mol Biol Cell* **6**:1423-1431.

Morrow VA, Foufelle F, Connell JM, Petrie JR, Gould GW, Salt IP. (2003) Direct activation of AMP-activated protein kinase stimulates nitric-oxide synthesis in human aortic endothelial cells. *J Biol Chem* **278**:31629-31639.

Ninomiya-Tsuji J, Kajino T, Ono K, Ohtomo T, Matsumoto M, Shiina M, Mihara M, Tsuchiya M, Matsumoto K. (2003) A resorcylic acid lactone, 5Z-7-oxozeaenol, prevents inflammation by inhibiting the catalytic activity of TAK1 MAPK kinase kinase. *J Biol Chem* **278**:18485-18490.

Ninomiya-Tsuji J, Kishimoto K, Hiyama A, Inoue J, Cao Z, Matsumoto K. (1999) The kinase TAK1 can activate the NIK-I kappaB as well as the MAP kinase cascade in the IL-1 signalling pathway. *Nature* **398**:252-256.

Nunes KP, Rigsby CS, Webb RC. (2010) RhoA/rho-kinase and vascular diseases: What is the link? *Cell Mol Life Sci* **67**:3823-3836.

Oka T, Hikoso S, Yamaguchi O, Taneike M, Takeda T, Tamai T, Oyabu J, Murakawa T, Nakayama H, Nishida K, Akira S, Yamamoto A, Komuro I, Otsu K. (2012) Mitochondrial DNA that escapes from autophagy causes inflammation and heart failure. *Nature* **485**:251-255.

Pyla R, Osman I, Pichavaram P, Hansen P, Segar L. (2014) Metformin exaggerates phenylephrine-induced AMPK phosphorylation independent of CaMKKbeta and attenuates contractile response in endothelium-denuded rat aorta. *Biochem Pharmacol* **92**:266-279.

Roberts TL, Dunn JA, Sweet MJ, Hume DA, Stacey KJ. (2011) The immunostimulatory activity of phosphorothioate CpG oligonucleotides is affected by distal sequence changes. *Mol Immunol* **48**:1027-1034.

Sakurai H, Miyoshi H, Toriumi W, Sugita T. (1999) Functional interactions of transforming growth factor beta-activated kinase 1 with IkappaB kinases to stimulate NF-kappaB activation. *J Biol Chem* **274**:10641-10648.

Salt IP and Hardie DG. (2017) AMP-activated protein kinase: An ubiquitous signaling pathway with key roles in the cardiovascular system. *Circ Res* **120**:1825-1841.

Shintani Y, Drexler HC, Kioka H, Terracciano CM, Coppen SR, Imamura H, Akao M, Nakai J, Wheeler AP, Higo S, Nakayama H, Takashima S, Yashiro K, Suzuki K. (2014) Toll-like receptor 9 protects non-immune cells from stress by modulating mitochondrial ATP synthesis through the inhibition of SERCA2. *EMBO Rep* **15**:438-445.

Shintani Y, Kapoor A, Kaneko M, Smolenski RT, D'Acquisto F, Coppen SR, Harada-Shoji N, Lee HJ, Thiemermann C, Takashima S, Yashiro K, Suzuki K. (2013) TLR9 mediates cellular protection by modulating energy metabolism in cardiomyocytes and neurons. *Proc Natl Acad Sci U S A* **110**:5109-5114.

Stacey KJ, Young GR, Clark F, Sester DP, Roberts TL, Naik S, Sweet MJ, Hume DA. (2003) The molecular basis for the lack of immunostimulatory activity of vertebrate DNA. *J Immunol* **170**:3614-3620.

Sung JY and Choi HC. (2012) Metformin-induced AMP-activated protein kinase activation regulates phenylephrine-mediated contraction of rat aorta. *Biochem Biophys Res Commun* **421**:599-604.

Szili D, Banko Z, Toth EA, Nagy G, Rojkovich B, Gati T, Simon M, Herincs Z, Sarmay G. (2014) TGFbeta activated kinase 1 (TAK1) at the crossroad of B cell receptor and toll-like receptor 9 signaling pathways in human B cells. *PLoS One* **9**:e96381.

Tostes RC, Traub O, Bendhack LM, Webb RC. (1995) Sarcoplasmic reticulum Ca2+ uptake is not decreased in aorta from deoxycorticosterone acetate hypertensive rats: Functional assessment with cyclopiazonic acid. *Can J Physiol Pharmacol* **73**:1536-1545.

Turkseven S and Ertuna E. (2013) Prolonged AMP-activated protein kinase induction impairs vascular functions. *Can J Physiol Pharmacol* **91**:1025-1030.

Veiko NN, Konorova IL, Neverova ME, Fidelina OV, Mkrtumova NA, Ershova ES, Kon'kova MS, Postnov AI. (2010) Delayed appearance of hypertension in spontaneously hypertensive rat (SHR) injected with CpG-rich DNA early in ontogenesis. *Biomed Khim* **56**:686-699.

Viollet B, Horman S, Leclerc J, Lantier L, Foretz M, Billaud M, Giri S, Andreelli F. (2010) AMPK inhibition in health and disease. *Crit Rev Biochem Mol Biol* **45**:276-295.

Vollmer J. (2006) TLR9 in health and disease. *Int Rev Immunol* **25**:155-181.

Vollmer J and Krieg AM. (2009) Immunotherapeutic applications of CpG oligodeoxynucleotide TLR9 agonists. *Adv Drug Deliv Rev* **61**:195-204.

Webb RC and Bhalla RC. (1976) Calcium sequestration by subcellular fractions isolated from vascular smooth muscle: Effect of cyclic nucleotides and prostaglandins. *J Mol Cell Cardiol* **8**:145-157.

Xie M, Zhang D, Dyck JR, Li Y, Zhang H, Morishima M, Mann DL, Taffet GE, Baldini A, Khoury DS, Schneider MD. (2006a) A pivotal role for endogenous TGF-beta-activated kinase-1 in the LKB1/AMP-activated protein kinase energy-sensor pathway. *Proc Natl Acad Sci U S A* **103**:17378-17383.

Xie M, Zhang D, Dyck JR, Li Y, Zhang H, Morishima M, Mann DL, Taffet GE, Baldini A, Khoury DS, Schneider MD. (2006b) A pivotal role for endogenous TGF-beta-activated kinase-1 in the LKB1/AMP-activated protein kinase energy-sensor pathway. *Proc Natl Acad Sci U S A* **103**:17378-17383.

Zheng B and Cantley LC. (2007) Regulation of epithelial tight junction assembly and disassembly by AMP-activated protein kinase. *Proc Natl Acad Sci U S A* **104**:819-822.

Zippel N, Malik RA, Fromel T, Popp R, Bess E, Strilic B, Wettschureck N, Fleming I, Fisslthaler B. (2013) Transforming growth factor-beta-activated kinase 1 regulates angiogenesis via AMP-

activated protein kinase-alpha1 and redox balance in endothelial cells. *Arterioscler Thromb Vasc Biol* **33**:2792-2799.

FOOTNOTES

This work was supported by the American Heart Association (Grants #13PRE14080019, #14POST20490292, and #15GRNT25700451); the National Institutes of Health National Heart, Lung, and Blood Institute (Grant P01HL134604); and the National Institutes of Health National Institute of General Medical Sciences (Grant K99GM118885).

FIGURE LEGENDS

Figure 1. TLR9 agonist ODN2395 increases phospho-AMPKα^{Thr172} expression in isolated arteries and vascular smooth muscle cells (VSMCs). Protein expression analysis was performed for phospho-AMPKα^{Thr172} normalized to total AMPKα in (A) mesenteric resistance arteries (MRA), (B) aorta, (C) endothelium denuded (E-) aorta, and (D) VSMCs incubated in either vehicle or ODN2395 (2 μmol/L), with and without ODN2088 (20 μmol/L). Protein expression analysis for (E) phospho-acetyl-CoA carboxylase (ACC)^{Ser79} normalized to total ACC was performed in VSMCs incubated in either vehicle or ODN2395, with and without compound C (10 μmol/L). *Above*, representative images of immunoblots; *below*, densitometric analysis. n=4-8. One-way ANOVA: *p<0.05 vs. vehicle.

Figure 2. TLR9 agonist ODN2395 does not impair SERCA2 activity, unlike classical SERCA2 inhibitor thapsigargin, nor does it promote TLR9-SERCA2 colocalization in vascular tissues. In denuded mesenteric resistance arteries (MRA) incubated in either vehicle, ODN2395 (2 μmol/L), or thapsigargin (1 μmol/L), contractile responses were measured during (A) calcium loading, (B) after intracellular calcium release, and (C) the time to achieve maximum relaxation after norepinephrine washout. ATP concentration was measured in isolated microsomes (n=5; 8 pooled aorta/sample), incubated in either vehicle or ODN2395, with or without thapsigargin, (D) across a 60 min time course and (E) summated as area under the curve (AUC). (F) Co-immunoprecipitation was performed for TLR9 with SERCA2 in MRA incubated with vehicle or ODN2395 (n=3; 2 pooled MRA/sample). (G) Protein expression analysis was performed for phospho-AMPKα^{Thr172} normalized to total AMPKα in MRA incubated with vehicle or thapsigargin. *Above*, representative images of immunoblots; *below*, densitometric analysis. n=3-

6. One-way ANOVA: *p<0.05 vs. vehicle; Two-way ANOVA: *p<0.05 vs. vehicle, #p<0.05 vs. ODN2395.

Figure 3. TLR9 agonist ODN2395-dependent phosphorylation of AMPKα is prevented by inhibiting TAK1 in vascular smooth muscle cells. Protein expression analysis was performed for (A) phospho-AMPKα^{Thr172} normalized to total AMPKα after incubation in either vehicle or ODN2395 (2 μmol/L), with and without (57)-7-oxozeaenol (100 nmol/L), (B) phospho-TAK1$^{Thr184/187}$ normalized to total TAK1 after incubation in either vehicle or ODN2395, with and without ODN2088 (20 μmol/L), (C) phospho-AMPKα^{Thr172} normalized to total AMPKα after incubation in either vehicle or ODN2395, with and without bafilomycin A1 (10 nmol/L), and (D) phospho-LKB1^{Ser428} normalized to total LKB1 after incubation in either vehicle or ODN2395, with and without (57)-7-oxozeaenol. *Above,* representative images of immunoblots; *below,* densitometric analysis. n=5-8. One-way ANOVA: *p<0.05 vs. vehicle.

Figure 4. TLR9 agonist ODN2395 increases filamentous (F)-to-globular (G) actin ratio in vascular smooth muscle cells. Quantitative protein expression analysis (A) was performed for F and G actin after incubation in either vehicle or ODN2395 (2 μmol/L). *Above*, representative images of immunoblots; *below*, densitometric analysis. Confocal microscopy (63X objective) (B) was also performed to observe F actin accumulation and organization, as well as immunofluorescence of paxillin, after incubation in either vehicle or ODN2395. n=4-5. Student's t-test: *p<0.05 vs. vehicle.

Figure 5. TLR9 agonist ODN2395 increases RhoA/ROCK activation via AMPKα to regulate actin polymerizing protein cofilin. (A) Concentration-response curves to Y-27632, with or without compound C (10 μmol/L), in denuded (E-) mesenteric resistance arteries (MRA) incubated with vehicle or ODN2395 (2 μmol/L). Protein expression analysis for (B) phospho-MYPT1^{Thr696} normalized to total MYPT1 was performed in vascular smooth muscle cells (VSMCs) incubated in either vehicle or ODN2395, with and without compound C and (C) phospho-cofilin^{Ser3} normalized to total cofilin was performed in VSMCs incubated in either vehicle or ODN2395, with and without Y-27632 (1 μmol/L). *Above*, representative images of immunoblots; *below*, densitometric analysis. n=4-5. Two-way ANOVA: *$p<0.05$ vs. vehicle, #$p<0.05$ vs. ODN2395; Student's t-test: *$p<0.05$ vs. vehicle; One-way ANOVA: *$p<0.05$ vs. vehicle.

Figure 6. Schematic summarizing TLR9-AMPKα signaling in vascular smooth muscle cells (VSMCs). Toll-like receptor 9 activation in VSMCs leads to the phosphorylation of AMPKα via TAK1, and activated AMPKα can subsequently trigger RhoA/ROCK, mediating the accumulation and disorganization of F actin.

JPET Fast Forward. Published on January 18, 2018 as DOI: 10.1124/jpet.117.245746
This article has not been copyedited and formatted. The final version may differ from this version.

Table 1.

Protein	Dilution	Secondary antibody	Company/catalog #
Phosphorylated AMPKα^{Thr172}	1:1000	Rabbit	Cell Signaling Technology /2535
Total AMPKα	1:1000	Rabbit	Cell Signaling Technology/2532
Phosphorylated ACC^{Ser79}	1:1000	Rabbit	Cell Signaling Technology/3661
Total ACC	1:1000	Rabbit	Cell Signaling Technology/3676
Phosphorylated TAK1$^{Thr184/187}$	1:1000	Rabbit	Thermo Fisher Scientific/MA5-15073
Total TAK1	1:1000	Rabbit	Cell Signaling Technology/4505
Phosphorylated MYPT1^{Thr696}	1:1000	Rabbit	Cell Signaling Technology/5163
Total MYPT1	1:1000	Mouse	BD Transduction Laboratories (San Jose, CA)/612165
Phosphorylated cofilin^{Ser3}	1:1000	Rabbit	Cell Signaling Technology/3311
Total cofilin	1:1000	Rabbit	Cell Signaling Technology/3318
Phosphorylated LKB1^{Ser428}	1:1000	Rabbit	Cell Signaling Technology/3482
Total LKB1	1:1000	Rabbit	Cell Signaling Technology/3047
β-actin	1:50,000	Mouse	Sigma-Aldrich/A3854

Table 1. Proteins probed for in Western blots. This table contains a list of the specific antibodies used in the current manuscript, including dilutions, secondary antibody host species, and company from which the antibody was purchased.

JPET Fast Forward. Published on January 18, 2018 as DOI: 10.1124/jpet.117.245746
This article has not been copyedited and formatted. The final version may differ from this version.

Figure 1.

(A) (B) (C) (D)

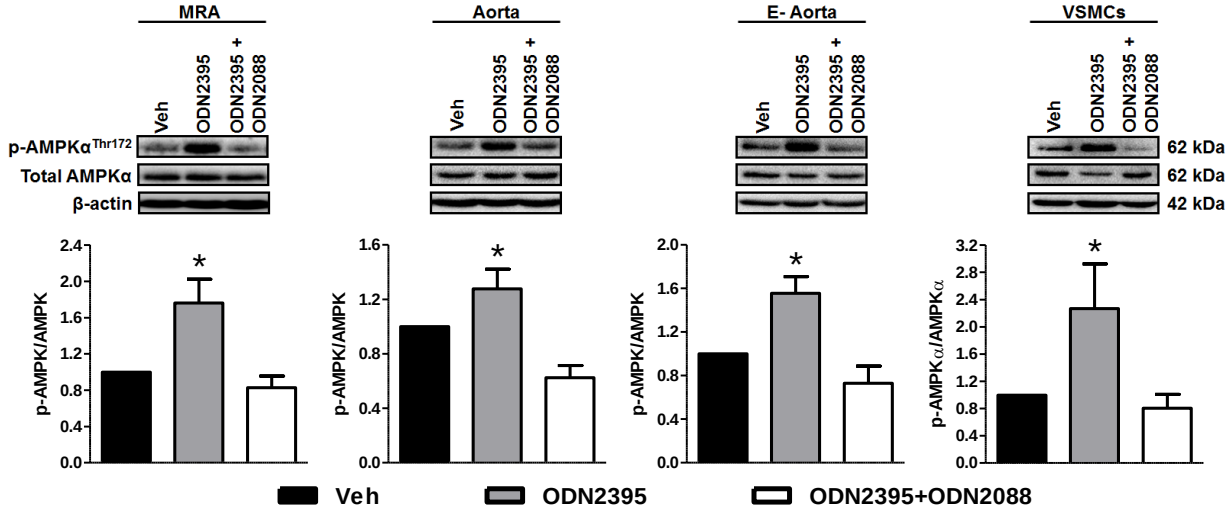

(E)

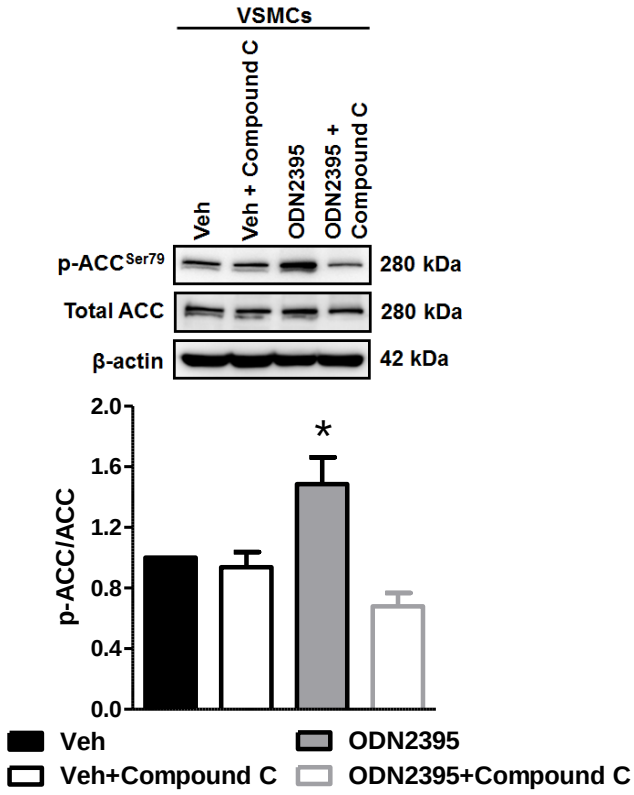

JPET Fast Forward. Published on January 18, 2018 as DOI: 10.1124/jpet.117.245746
This article has not been copyedited and formatted. The final version may differ from this version.

Figure 2.

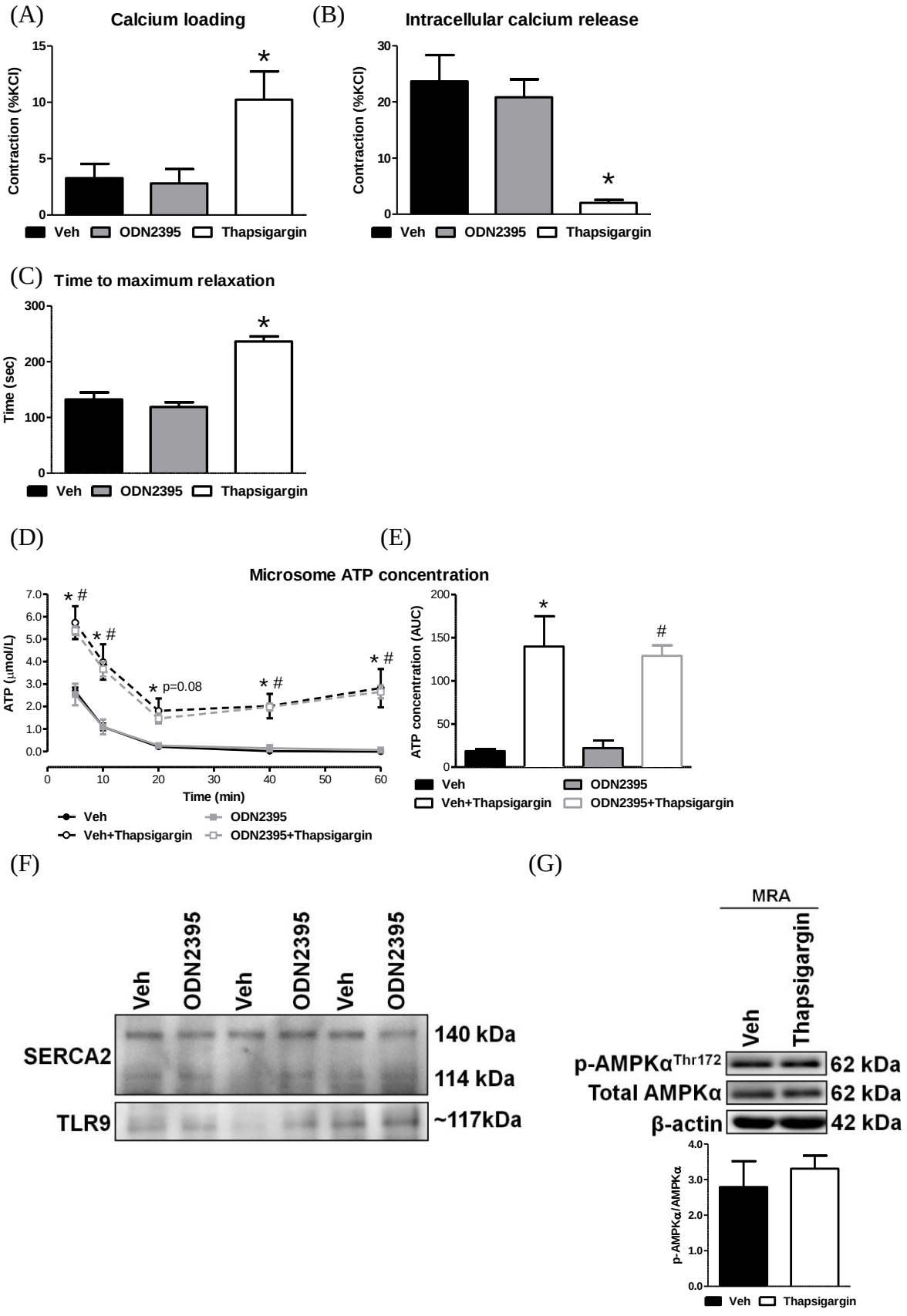

JPET Fast Forward. Published on January 18, 2018 as DOI: 10.1124/jpet.117.245746
This article has not been copyedited and formatted. The final version may differ from this version.

Figure 3.

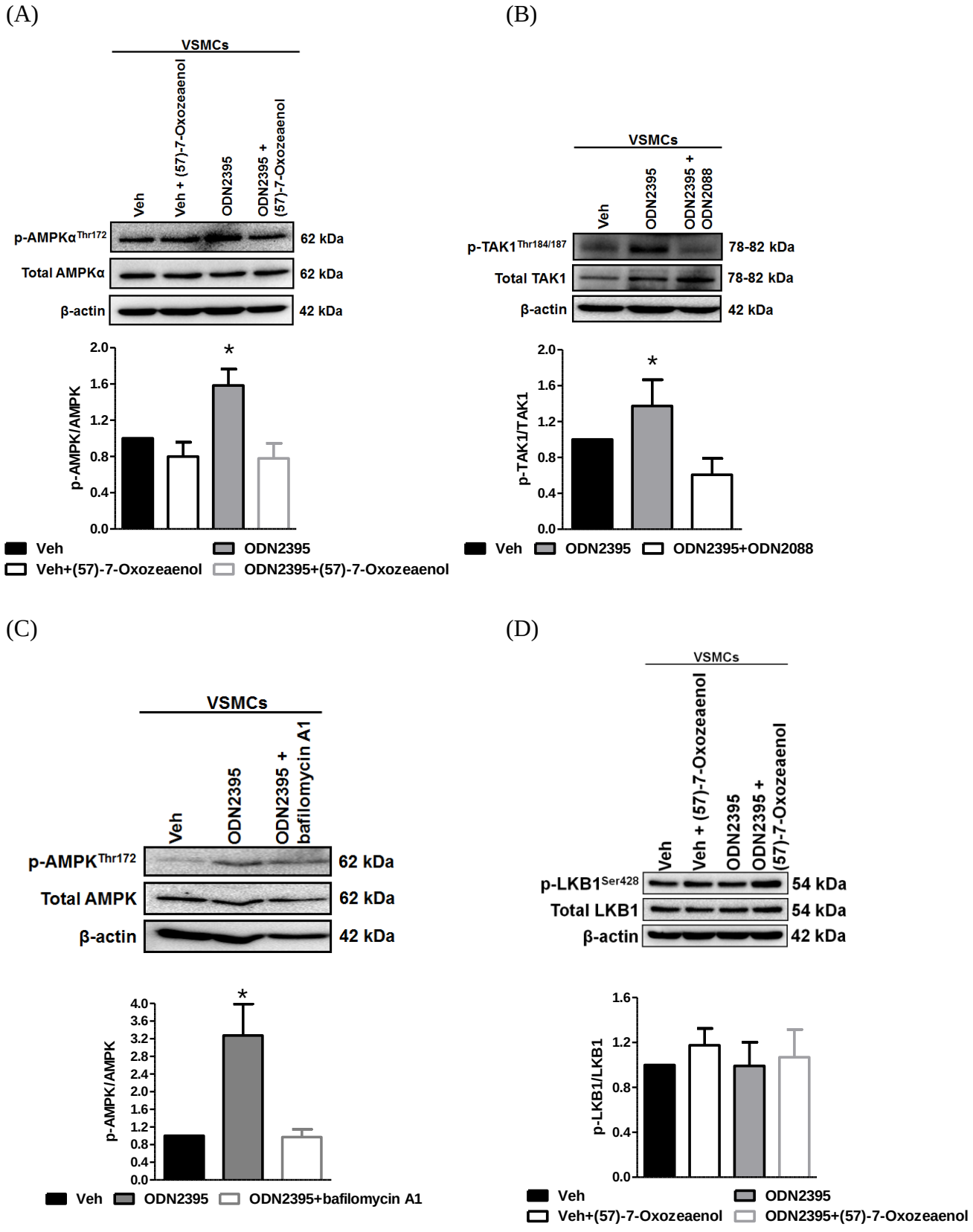

JPET Fast Forward. Published on January 18, 2018 as DOI: 10.1124/jpet.117.245746
This article has not been copyedited and formatted. The final version may differ from this version.

Figure 4.

(A)

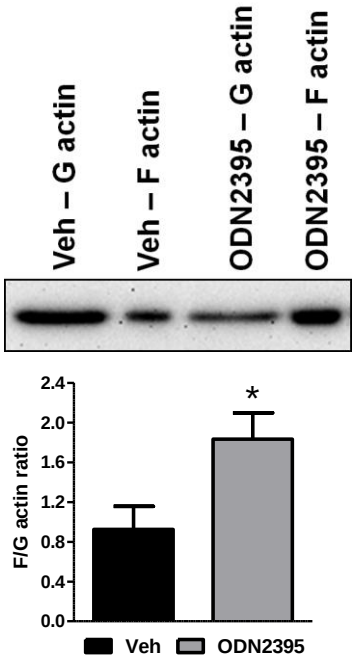

(B)

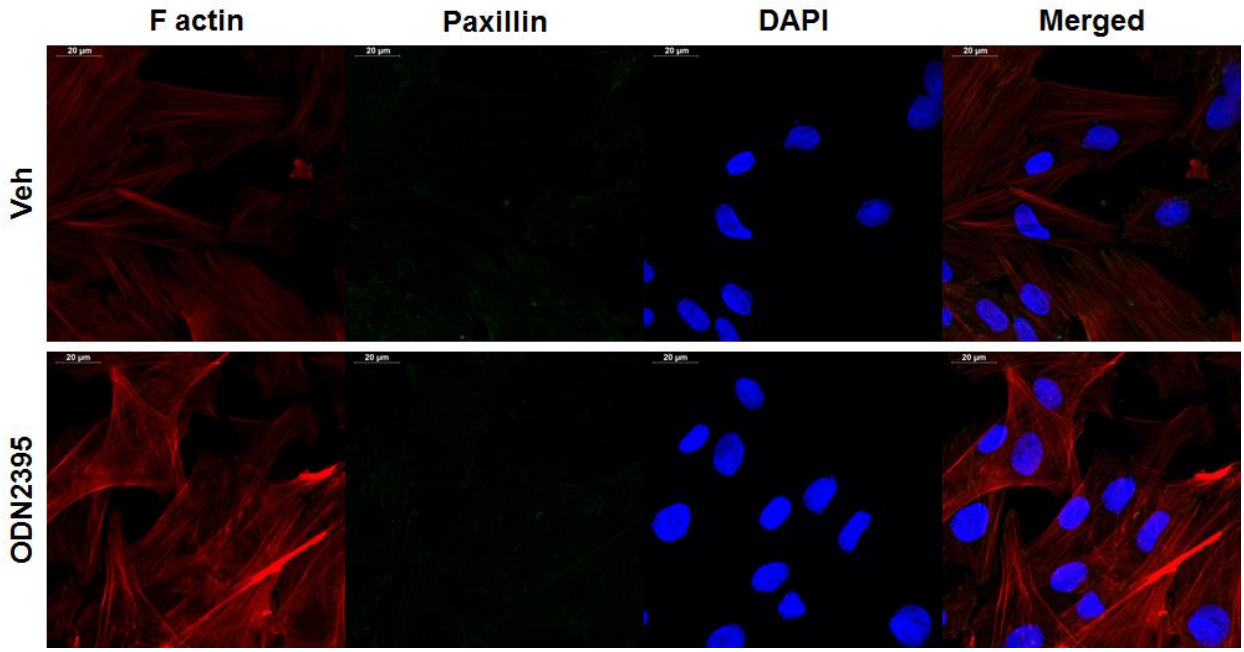

JPET Fast Forward. Published on January 18, 2018 as DOI: 10.1124/jpet.117.245746
This article has not been copyedited and formatted. The final version may differ from this version.

Figure 5.

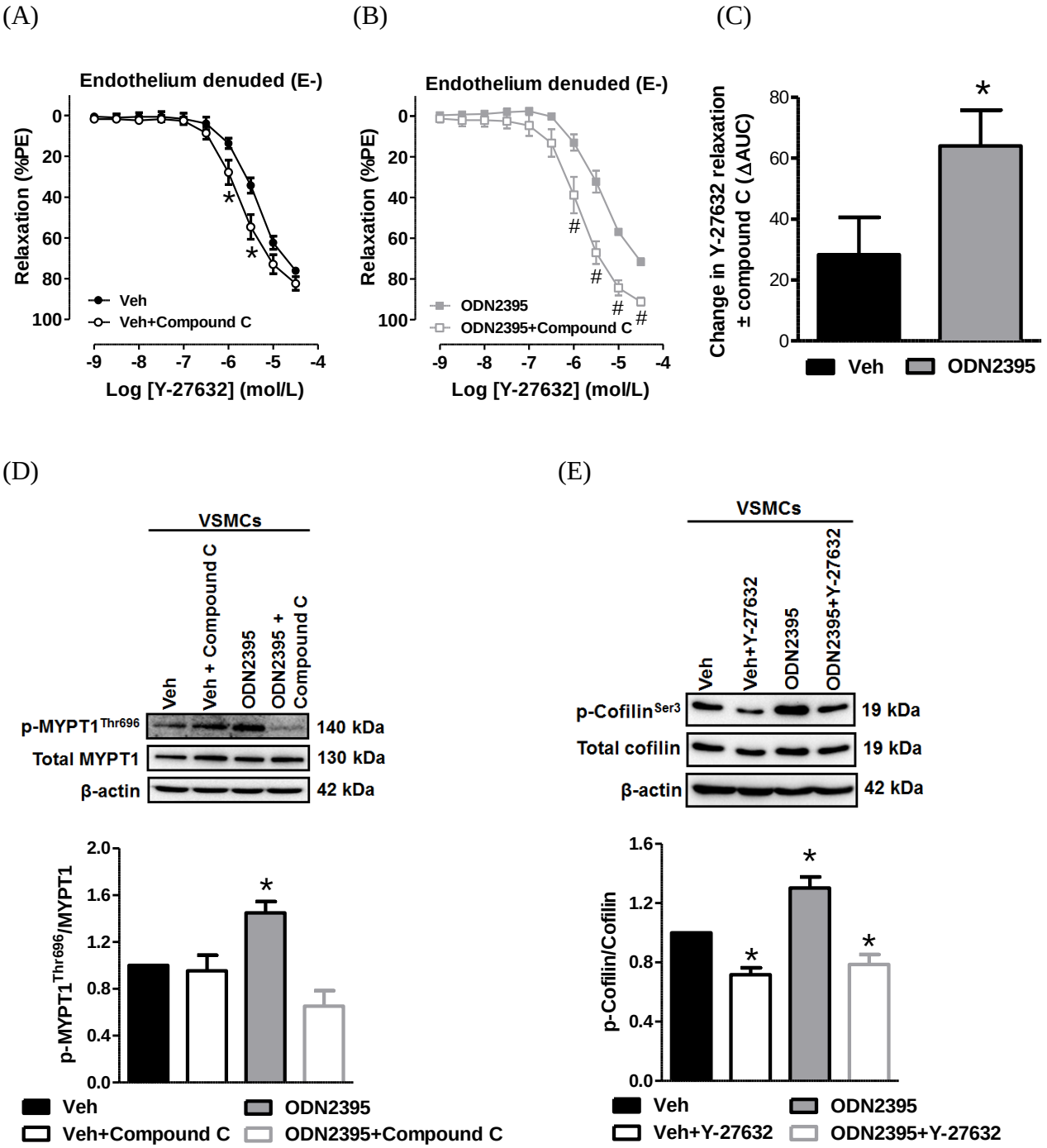

JPET Fast Forward. Published on January 18, 2018 as DOI: 10.1124/jpet.117.245746
This article has not been copyedited and formatted. The final version may differ from this version.

Figure 6.